Supplementary Information For

Bidentate forms of β-triketimines: syntheses, characterization and outstanding performance of enamine-diimine cobalt complexes in isoprene polymerization

Mohammed N. Alnajrani‡* and Francis S. Mair*

Organic Materials Innovation Centre (OMIC), School of Chemistry, The University of Manchester, Brunswick Street, Manchester M13 9PL. E-mail: mair@manchester.ac.uk. ‡*King Abdulaziz City for Science and Technology (KACST), Kingdom of Saudi Arabia, PO Box 6086, Riyadh 11442. E-mail: mnajrani@kacst.edu.sa*

Contents

1 Kinetic study

The polymerization of isoprene by **I** (Figure 1.a) and **II** (Figure 2.a) were first order with respect to the monomer. In the case of **I**, *k* was found to be 1.29 x 10^{-3} s^{-1} which means that the value of propagation rate (R_p) becomes 1.84 x 10^{-3} M s^{-1}. After 20 minutes, more than 75% of isoprene was converted and after that the rate of conversion reduced due to the low concentration of isoprene in the solution as can be seen in Figure 1.b.

In the case of **II**, the value of *k* was found to be 0.17 h^{-1} (≈ 4.7 x 10^{-5} s^{-1}) leading the value of R_p to be 6.75 x 10^{-5} M s^{-1}. In addition, after 6 hours where around 65% of isoprene was converted, propagation rate slowed down because of the reduction of isoprene concentration (Figure 2.b).

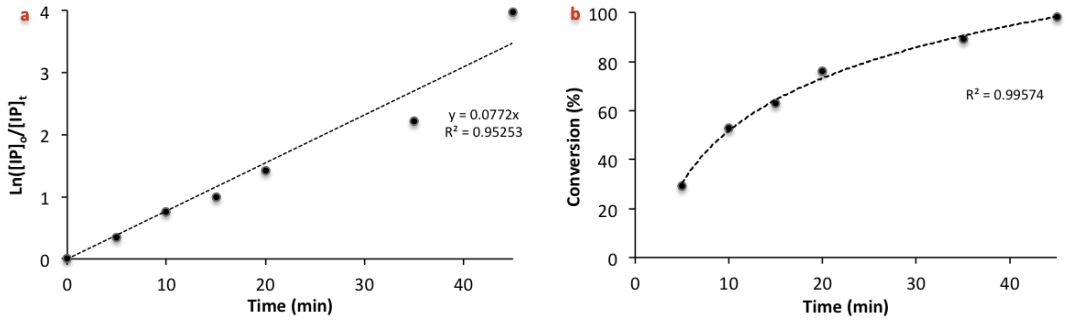

Figure 1 First-order kinetic plot for polymerization of IP by I: a) $\ln([IP]_0/[IP]_t)$ *vs.* time; b) Conversion *vs.* time.

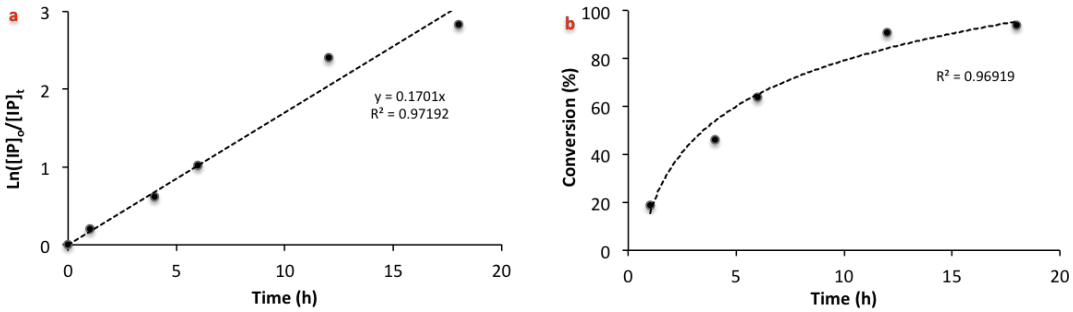

Figure 2 First-order kinetic plot for polymerization of IP by II: a) $\ln([IP]_0/[IP]_t)$ *vs.* time; b) Conversion *vs.* time.

2 The presence of chain transfer in IP polymerization by I

The molecular weights increased linearly with time where more than 98.1% of the monomer was consumed (Figure 3). In isolation, this could be taken as evidence of a living polymerization; however, the regular increase in M_w and M_n even as monomer consumption approached 100% suggests that the linearity is the result of accidental cancellation of two or more opposing parameters, such as chain transfer to monomer, which would tend to limit the growth of M_n with time, and chain transfer to polymer, which would tend to increase M_n substantially. However, the lines do not pass through the origin, and dispersity values are close to the most probable distribution, 2, even at relatively short reaction times. This value increases relatively slowly, though at longer reaction times, dispersity broadens further, as the effects of chain transfer to polymer produce some crosslinking. Although there was an increase in the value dispersity, the variation was small. The data appear to fit the assumption of some chain transfer, and the increase in the number of chains seems to suggest this is to monomer (*vide infra*), but its rate is slow compared to the rate of propagation, and hence M_n and M_w increase with time.

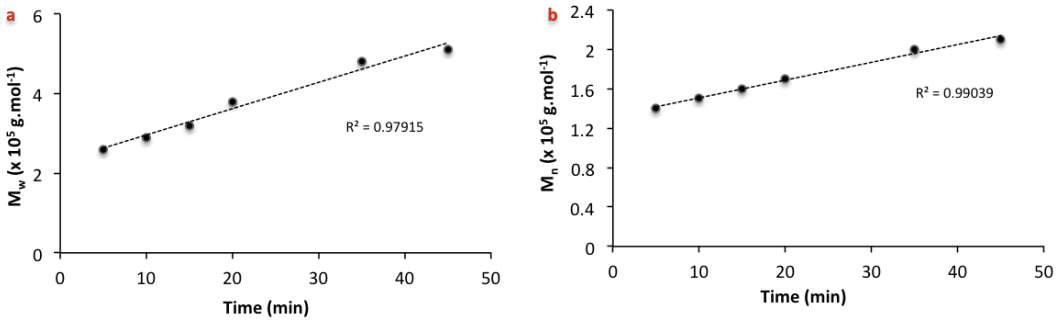

Figure 3 Polymerization behaviour: a) M_w *vs.* time; b) M_n *vs.* time.

There are several types of chain transfer which can happen to monomer, aluminium or polymer chain. The key intermediates in these three processes are shown in Chart 1. At the beginning of the polymerization, the concentration of the monomer was high and the propagation rate was much faster compared to the rate of the chain transfer to monomer. If we assume that at early conversion, chain transfers are to monomer only, then it is possible to extract a rate for this (equation 1)

$$R_{ctm} = k_{ctm}[IP]\,[C^*] \ldots\ldots\ldots (1)$$

Where R_{ctm} = rate of chain transfer to monomer, k_{ctm}= rate constant for chain transfer to monomer and [IP] is the concentration of isoprene.

In order to investigate the rate of chain transfer to monomer, it was required to calculate the number of chains (N_c) which increased with the presence of chain transfer to monomer. Therefore, N_c was calculated from Equation 2 and then was plotted against polymerization time. It was noticed that the number of chains increased linearly at the beginning of the polymerization where the monomer was plentiful. At higher conversion, N_c levelled off due to the absence of chain transfer to monomer (Figure 4.a) as monomer dwindled. The first four datapoints fitting to straight line were used in order to measure the rate of chain transfer to monomer (R_{ctm}). Therefore, the same graph was potted with just the first four datapoint and the R_{ctm} was equal to the gradient; 30.88×10^{16} chains min^{-1} (51.46×10^{14} chains s^{-1}). (Figure 4.b). This rate is higher compared to that found in our previous study on tridentate precatalysts (4.81×10^{14} chains s^{-1}).[1]

$$\text{no. of chains at time t } (N_C) = \frac{\text{yield at time t (g)}}{M_n\ (\text{g.mol}^{-1})} \times \text{ Avogadro number}(\text{mol}^{-1}) \ldots\ldots\ldots(2)$$

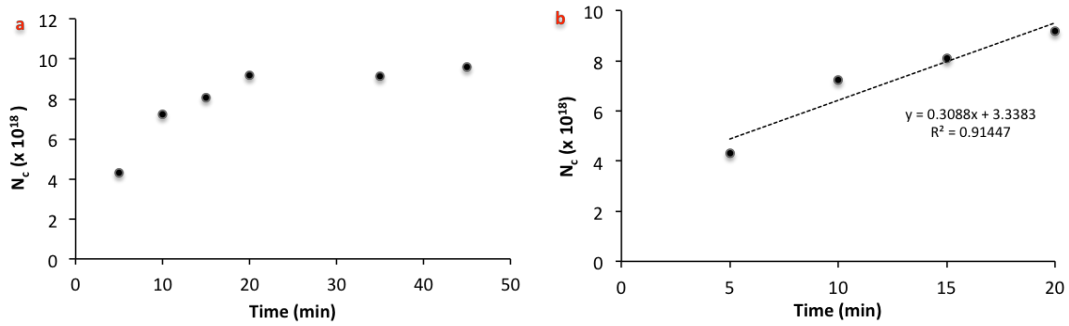

Figure 4 Plotting of N_c against time.

However, if instantaneous initiation is assumed, then the value of N_c at zero conversion is equal to the number of active centres (C*), since there was no opportunity for chain transfer. This phenomenon was described by Boucher *et al.*[2] In support of the assumption of rapid initiation, a rapid colour change was observed

immediately upon addition of DEAC. Therefore, conversion was plotted against N_c, which increased linearly with conversion until 75% of isoprene monomers were converted. N_c then levelled off indicating the reduction of chain transfer to monomer (Figure 5.a), as should be expected in a polymerisation with depleting monomer. In this case, the initial behaviour is key, where chain transfer to monomer is dominant; therefore the graph was plotted again using just the first four datapoints (Figure 5.b). The number of active centres was obtained as the intercept at zero conversion of the linear portion of the plot of N_c *vs*. conversion. Consequently, C* of **I** was 13.817×10^{17}, in which cases [C*] can be calculated according to equation 3 to be 6.6×10^{-5} M. Since the concentration of cobalt catalyst added was 5 µmol in 35 mL, i.e. [Co] = 14.3 x 10^{-5} M, this shows that approximately 46% of cobalt present was active.

$$[C^*] = \frac{C^*}{\text{Avogadro number}(\text{mol}^{-1})} \div 0.035\ (\text{L}) \ldots\ldots\ldots (3)$$

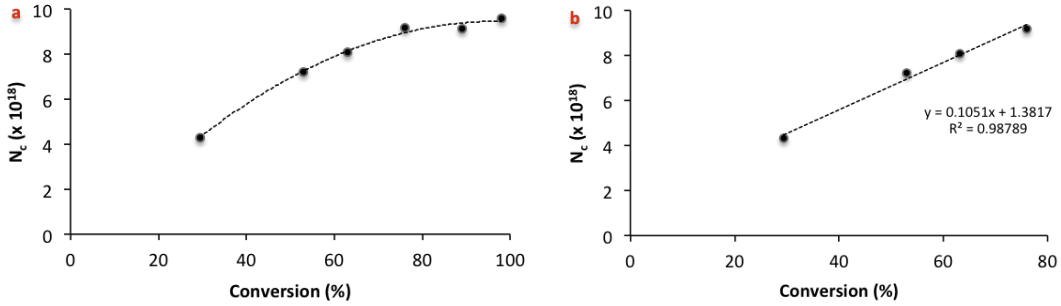

Figure 5 Plotting of N_c against conversion.

The possibility of chain transfer to polymer increases as the concentration of monomer reduces. At the beginning of the polymerization the molecular weight distribution was monomodal whereas it became bimodal after 45 minutes, at which point more than 98% of the monomer was consumed (Figure 6). Initially the active sites preferred to insert new monomer rather than react to the main-chain alkenes of 1,4-enchained units or more likely, side-chain alkenes of 3,4-enchained units; Chart 1. Whereas, the chain transfer to polymer becomes more probable as the monomers dwindled at high conversion. Hence, a high M_w tail developed in the distribution.

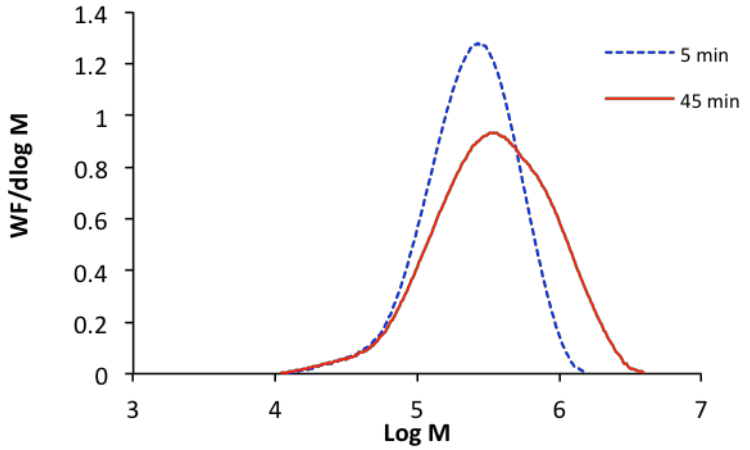

Figure 6 GPC curves of Polyisoprene by I/DEAC; for 5 and 45 minutes.

If the polymerization was left for extended periods after all monomers were consumed, would the chain transfer to polymer continue and lead to higher degree of crosslinking? To answer the query further polymerizations were carried out for sufficient time to achieve complete conversion. When the complete polymerization was left for two further hours the molecular weight distribution of the obtained polymer was broad and bimodal (Figure 7). Although there was chain transfer to polymer, its rate was slow, and so the degree of crosslinking was low, so that all of the polymer was soluble in THF. In order to obtain high degrees of crosslinking the polymerization needed to be left for days, after which the obtained polymer was insoluble in any organic solvent. This process could of course be accelerated by heat, or by additives, as in more conventional vulcanization.

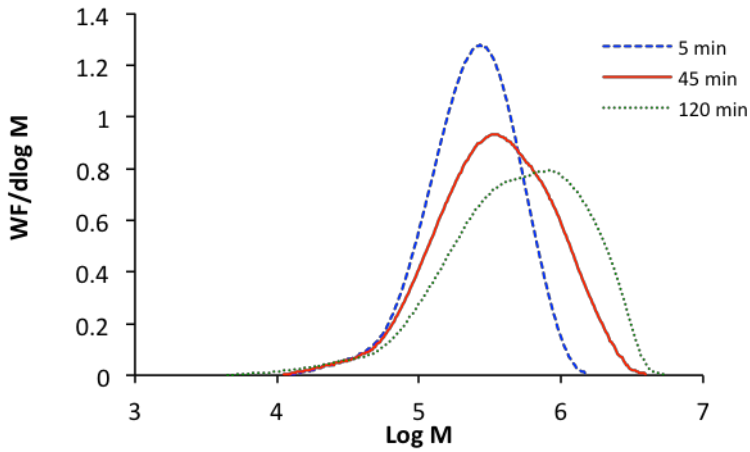

Figure 7 GPC curves of Polyisoprene by I/DEAC; for 5, 45 and 120 minutes.

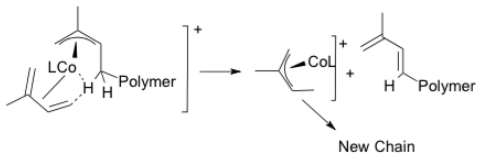

Direct Chain Transfer to Monomer

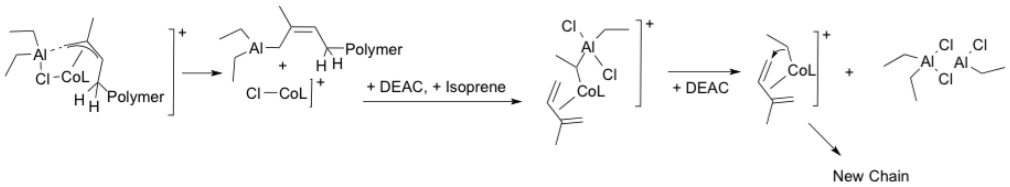

Chain Transfer to Aluminium

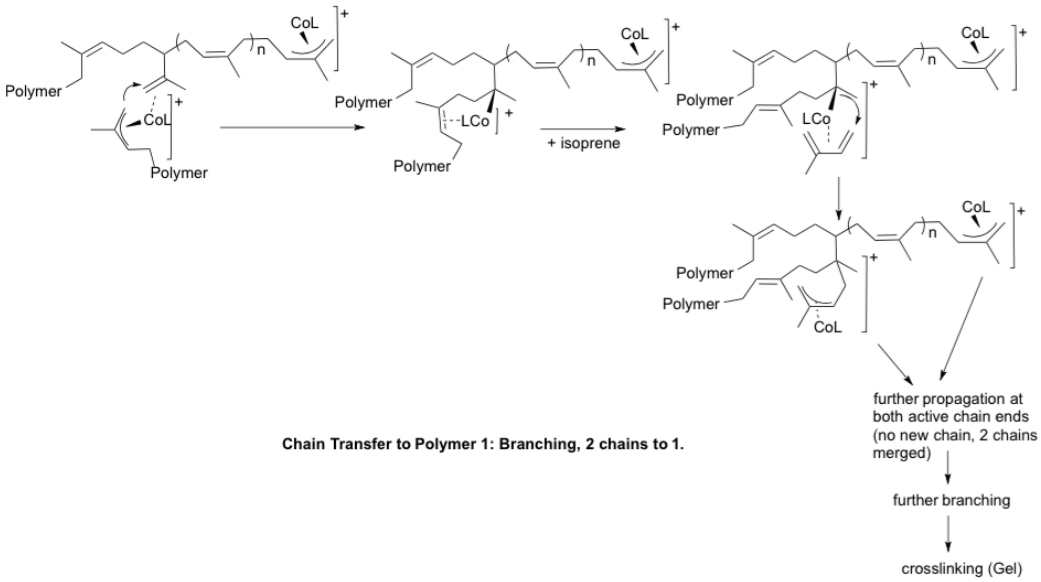

Chain Transfer to Polymer 1: Branching, 2 chains to 1.

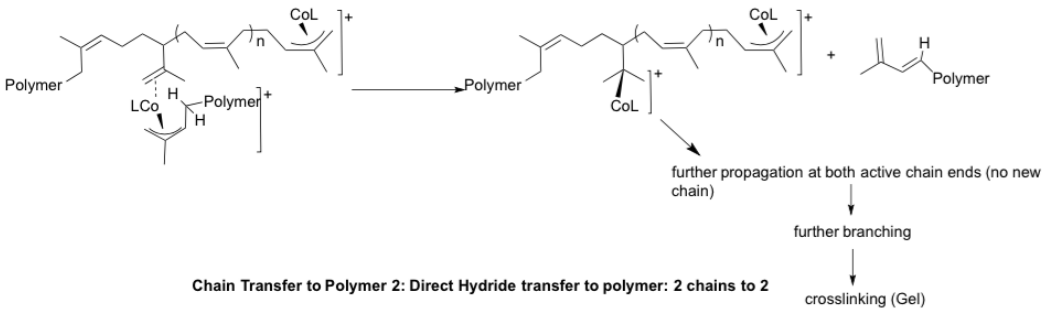

Chain Transfer to Polymer 2: Direct Hydride transfer to polymer: 2 chains to 2

Chart 1 Chain transfer processes.

3 The presence of chain transfer in IP polymerization by II

In the case of **II**, the behaviour was similar, but all processes were much slower compared with **I**. For example, the molecular weight increased slowly for the first 12 hours while polydispersity increased from 2.38 to 3.10 indicating the presence of chain transfer to monomer. With greater time periods elapsed, the distribution of molecular weights was wider than that found for **I**. However, it was still monomodal for the first 12 hours and became broader and multimodal after 12 hours. The molecular weight then jumped at the end of the polymerization where chain transfer to polymer took place (Figure 8).

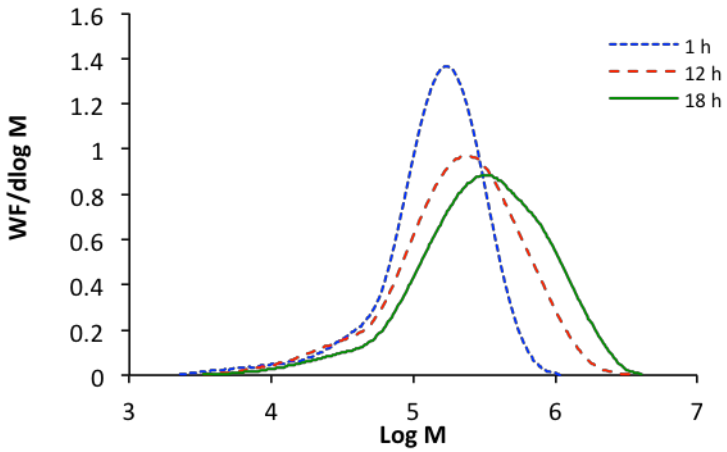

Figure 8 GPC curves of Polyisoprene by II/DEAC.

Investigation of the number of chains was calculated for **II** as has already been presented for **I** here. It was found, as for **I**, that the number of chains increased at the beginning of the polymerization where chain transfer to monomer dominated. At the end of the polymerization, again as for **I**, there was a drop in the number of chains due to crosslinking (chain transfer to polymer) (Figure 9.a). The first three datapoints fitting to straight line were used in order to measure the rate of chain transfer to monomer (R_{ctm}). Therefore, the same graph was potted with just the first three datapoints, where R_{ctm} was equal to the gradient; 1.9×10^{18} chains h^{-1} (5.37×10^{14} chains s^{-1}) (Figure 9.b).

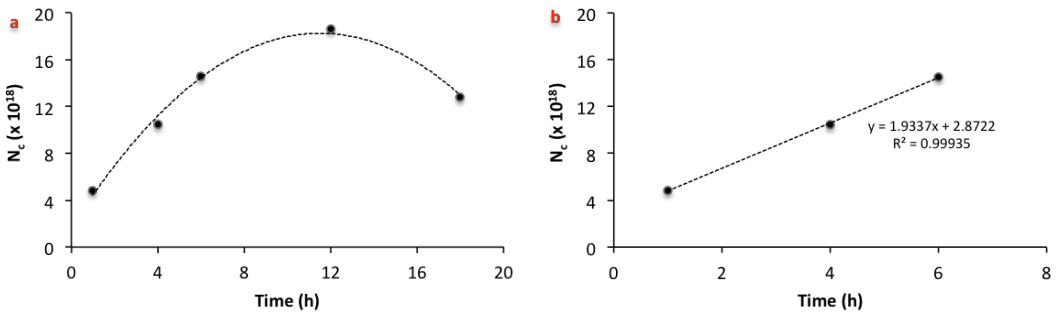

Figure 9 Plotting of N_c against time.

As mentioned earlier, the value of N_c at zero conversion is equal to the number of active centres (C*). Therefore, conversion was plotted against N_c which increased linearly with conversion until 91% of isoprene monomer was converted, then N_c reduced indicating the dominance of chain transfer to polymer (Figure 10.a). The graph was plotted again using just the first four datapoints (Figure 10.b). With the assumption that at the early stages of conversion, transfer to monomer was dominant over transfer to polymer, the number of active centres was obtained as the intercept at zero conversion of the linear portion of the plot of N_c *vs*. conversion. Consequently, C* of **II** was 14.944×10^{17} which means 50% of cobalt complex was activated. This value is closely similar to that reported earlier for **I** (46%), and so there was negligible difference in the percentage of the active cobalt sites between **I** and **II**, but there was a remarkable difference in the activity, due to the much larger BArF ion forming a much looser ion-pair with the cobalt complex cation than those formed with the aluminium centred anions due to the nature of counter-ion as mentioned before.

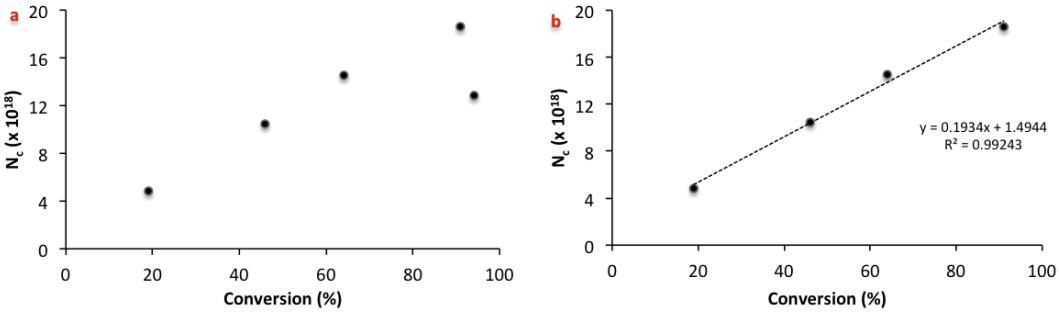

Figure 10 Plotting of N_c against conversion.

4 Influences of co-catalyst and [Al]/[Co] mol ratio

4.1 [L-Co-Br.THF][BArF] (I)

The activity of **I** was clearly influenced by the co-catalyst. Although EASC/**I** was more active (100%) compared to DEAC/**I** (52.9%) under the same conditions, the molecular weight of the produced polymer was lower (4.0×10^4 g mol^{-1}) and the molecular weight distribution was higher (5). This suggests that the higher degree of chlorine substituents facilitated chain transfer to aluminium (Chart 1).[3] The molecular weight distributions of the polymers produced by these two systems are displayed in Figure 11. Inspection of the molecular weight distribution reveals both a small M_w tail and a high M_w tail, suggesting the presence of chain transfer to monomer and perhaps to Aluminium (low M_w tail) and to polymer (high M_w tail) in the case of the **I**:EASC system. On the other hand, the **I**/DEAC system produced a polymer with narrow and monommodal distribution indicating that the chain transfer is lower compared to EASC system. Consequently, the increased Lewis acidity of the aluminium induced by the greater proportion of chlorine ligands facilitates chain transfer processes.

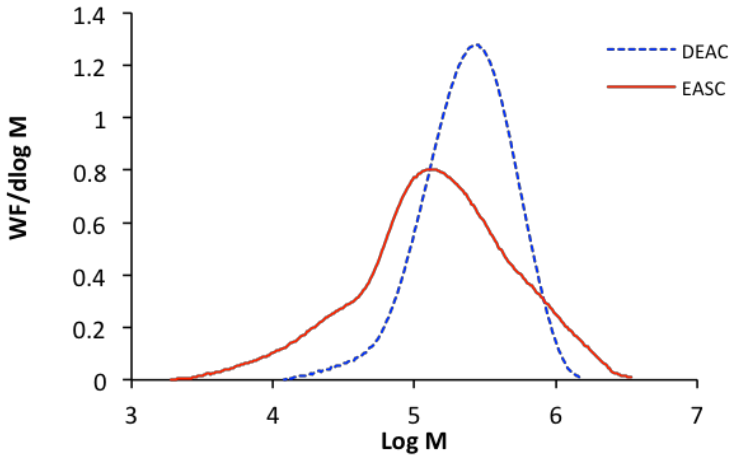

Figure 11 GPC curves of polyisoprene by I/DEAC and I/EASC systems.

The hypothesis that the high M_w tail appeared as a result of chain transfer to polymer events dominating at high conversion was tested by stopping the polymerization at lower conversion and determining the M_w distribution. The polymerization was carried for 1 minute. No high molecular weight tail was introduced to the distribution (M_w = 2.0×10^5 g mol^{-1} and M_n = 0.4×10^5 g mol^{-1}) and only a small molecular

weight tail presented (Figure 12). The observations are consistent with the hypothesis. Furthermore, leaving the polymerization for 24 h resulted in a very high molecular weight tail and produced a polymer which proved difficult to pass through the GPC filter (pore size = 0.45 μm). In addition, the high molecular weight tail was bigger after 24 hours compared to 10 minutes. This means that chain transfer to polymer was happening. Due to the relatively low degree of crosslinking at short times, the produced polymer was soluble in THF. However, the produced polymer of a polymerization left for 48 h was insoluble in any organic solvent.

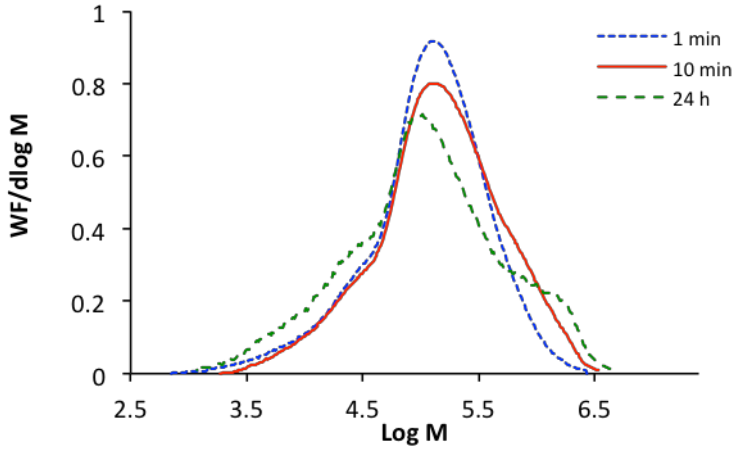

Figure 12 GPC curves of polyisoprene by I/EASC systems for different time.

Al/Co mol ratio remarkably played an important role in both the activity and the molecular weight. For example, the conversion was 26.8 % with M_w of 2.8 × 10^5 g mol^{-1} when Al/Co was 25:1, while increasing the ratio to 200:1 led to an increase of conversion to 93.8% and of M_w to 4.5 × 10^5 g mol^{-1}. This behaviour might be ascribed to increasing the number of active centres by increasing Al ratio. On the other hand, as Al:Co mol ratio was increased to 400:1, both the activity and the molecular weight dropped to 76.8% and 3.8 × 10^5 g mol^{-1} indicating deactivation of the active centre[4] as can be seen in Figure 13.

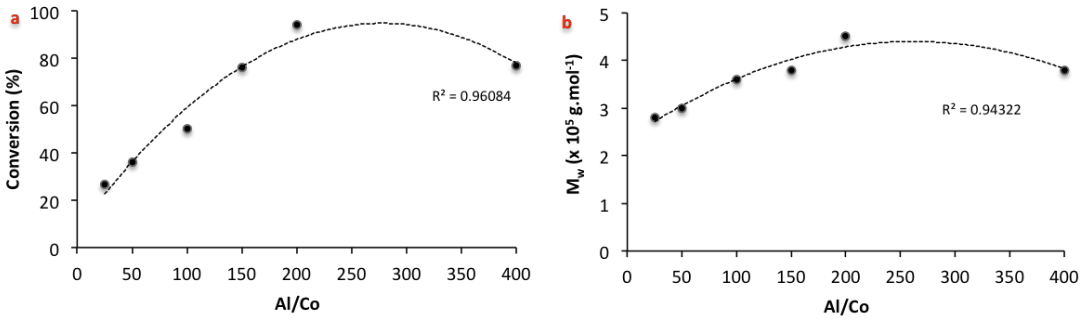

Figure 13 a) Conversion by I *vs.* Al:Co ratio; b) M_w of polyisoprene by I *vs.* Al:Co ratio.

Further investigation was required in order to find the effect of Al:Co ratio on both activity and molecular weight. Therefore, the number of chains (N_c) with different Al ratio was calculated and it was plotted against Al:Co mol ratio (Figure 14.a). It was found that N_c increased linearly as the Al ratio increased from 25 to 200 where also the activity increased. Consequently, this observation supports the above suggestion that the activation stage was more efficient and resulted in more active sites when Al ratio was 200. Further increment of Al:Co mol ratio resulted in deactivation of the active centres and therefore the number of chains dropped as can be seen in Figure 14.b.

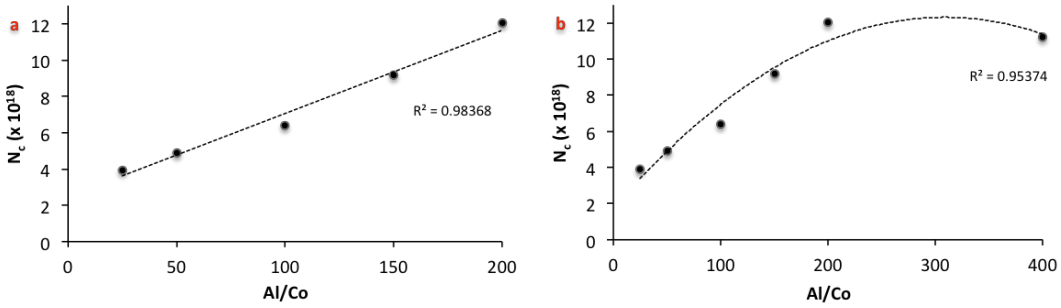

Figure 14 Plotting of N_c against Al/Co.

4.2 [LCoBr$_2$] (II)

As for **I**, EASC/**II** was more active than DEAC/**II** (97.3% and 19.0 % respectively) while the molecular weight was seven times lower for EASC/**II** (2.0×10^4 g mol^{-1}) compared to DEAC/**II** (8.0×10^4 g mol^{-1}). This huge difference in the molecular weight is attributed to much more rapid chain transfer with EASC. However, the large values of dispersity can be best explained by assuming that a range of active sites of

different propagation and chain transfer rates was present. This is readily rationalised when one considers that there are a range of counterions $[Al]^-$, and that each ion pair will behave differently.

As mentioned before for **I**, at the beginning of the polymerization using **II** where monomer was plentiful the chain transfer to monomer can be assumed to dominate, though chain transfer to aluminium also is likely. Using DEAC as co-catalyst, the molecular weight distribution shows a small molecular weight tail (Figure 15). On the other hand, use of EASC produced polyisoprene with a broad, trimodal distribution, with both low and high M_w peaks, in addition to the main peak at high conversion. As for **I**, the data was interpreted in terms of a low M_w peak resulting from chain transfers to Aluminium or monomer, and a high M_w peak resulting from chain transfers to polymer. To probe these assumptions, further polymerizations were carried out by EASC/**II** for shorter reaction times and then stopped where the monomer in the polymerization solution was plentiful (Figure 16). The data, and its interpretation, are exactly as for **I**, though the timescales are extended, and the broadening is more serious for this reason. Therefore, the rate of chain transfer to polymer was slow compared to chain transfer to monomer.

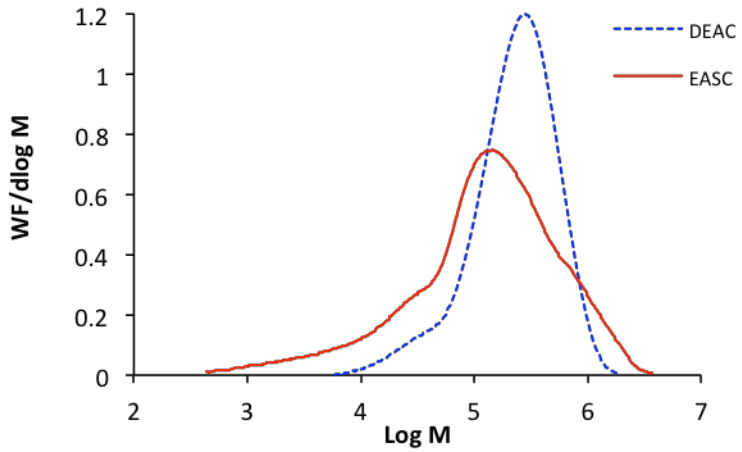

Figure 15 GPC curves of polyisoprene by II/DEAC and II/EASC systems.

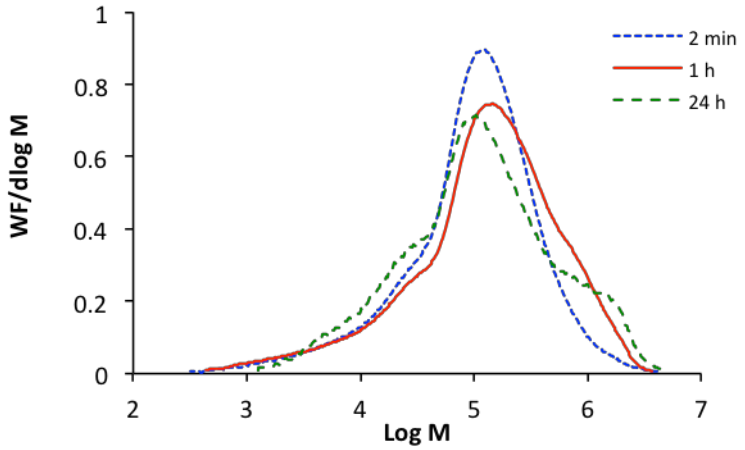

Figure 16 GPC curves of polyisoprene by II/EASC systems for different time.

In contrast with **I**, the activity of **II** decreased as the Al:Co mol ratio increased from 25 to 150. This is presumably because contact ion pair equilibria, where contact ion pairs are inactive forms of the catalytic site, were becoming saturated by additional free aluminium reagent. In addition, the molecular weight and molecular weight distribution also decreased slightly with increasing the Al/Co, but this is probably a function of the fact that at low ratio over the 6-hour reaction time the polymer reached full conversion and then began crosslinking, raising dispersity, M_n and M_w, but lowering the number of chains (N_c). Consequently, the lowest value of N_c was in the case of an Al:Co ratio of 25 (Figure 17.a). The value of N_c decreased as the ratio of Al increased from 50 to 150 (Figure 17.b) and the activity dropped. This phenomenon is ascribed to catalyst site deactivation.

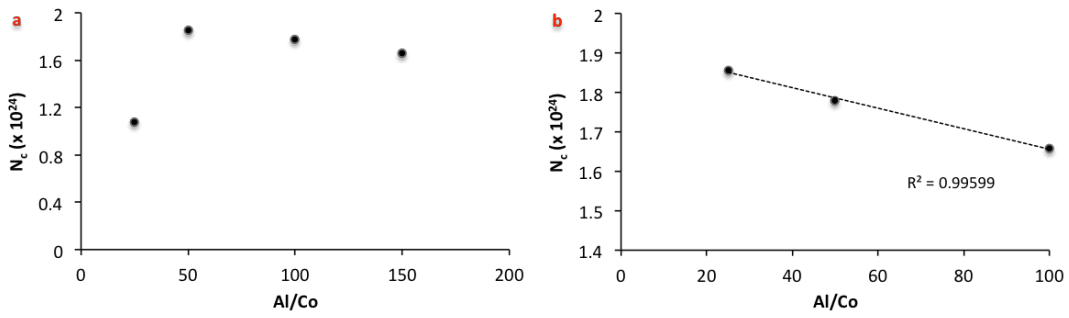

Figure 17 Plotting of N_c against Al/Co.

5 Influences of polymerization temperature:

5.1 [L-Co-Br.THF][BArF] (I)

The activity of **I** remarkably increased as the temperature increased from 0 to 70 °C indicating that **I** obeys Arrhenius rate behaviour. In addition, this observation might also be ascribed to the number of active centres (C*), which increased with polymerization temperature indicating the activation and chain transfer was more efficient at high temperature. In addition, the viscosity of the solution might have an influence; this means the viscosity value decreased with the temperature leading the chains to have more ability to move. Consequently, the rate of inserting the monomers would be higher, especially at the high molecular weight stage of a polymerization. It has been reported that at high polymerization temperature cobalt complexes suffer from decay of the active centre.[5] [6] Similar behaviour was observed in the present study; the activity of **I** decreased to 59.7% conversion at 100 °C (Figure 18.a).

However, the value of M_n was strongly affected by the polymerization temperature. M_n initially increased as the temperature increased, to an optimum value of 1.8×10^5 g mol^{-1} at 35 °C. Further increase in the temperature resulted in decrease of M_n to 8.0×10^4 g mol^{-1} at 100 °C, suggesting the presence of chain transfer.[7] Consequently, the effect of temperature on the number of chains (N_c) was plotted. N_c increased with temperature to an optimum value at 70 °C before dropping at 100 °C because of deactivation (Figure 18.b).

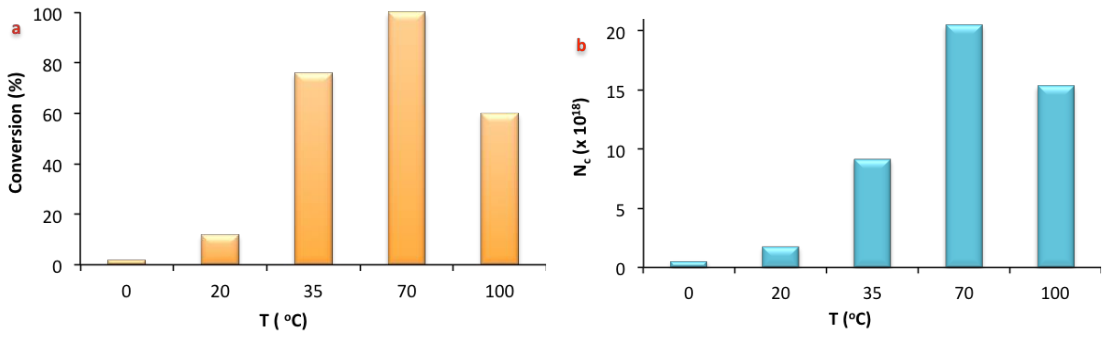

Figure 18 The effect of the polymerization temperature on :a) the activity and b) N_c using I.

The influence of temperature on the selectivity of polymerization is displayed in Figure 19. Behaviour identical to that previously reported for β-triketimine cobalt(II) complexes,[1] where *trans*-1,4-enchaiment was presented at low temperature while

increasing the temperature led to its disappearance and increased *cis*-1,4-enchaiment and 3,4-enchaiment, was found. This difference in the microstructure is ascribed to isomerization between *syn* and *anti* forms (see main text for full discussion).

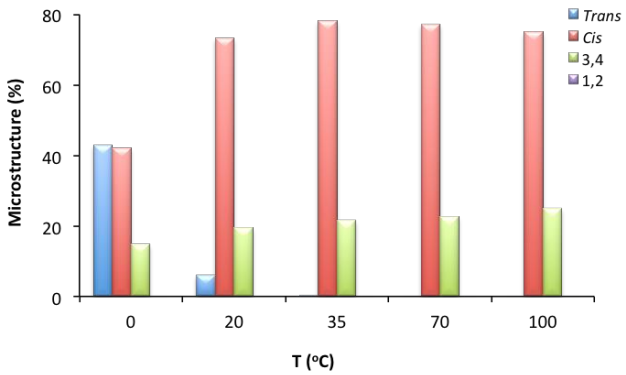

Figure 19 The effect of polymerization temperature on the selectivity of I.

5.2 [LCoBr2] (II)

The activity of **II**; as for **I**, increased linearly ($r^2 = 0.96$) as the temperature increased from 0 to 70 °C, while further increase led to reduction in the activity due to deactivation of active centres (Figure 20.a). The value of N_c was found to increase linearly ($r^2 = 0.97$) as the temperature increased from 0 to70 °C and then drop at 100 °C due to chain transfer to polymer events, and catalyst deactivation events (Figure 20.b), exactly as found for **I**.

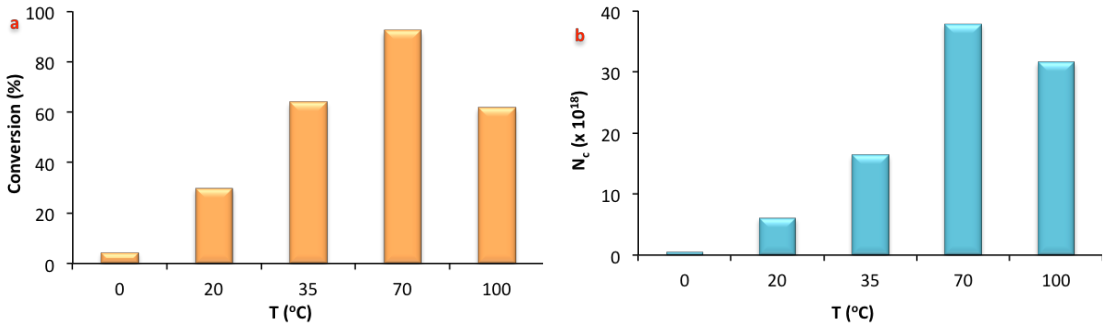

Figure 20 The effect of the polymerization temperature on :a) the activity and b) N_c using II.

Molecular weight decreased with the increase of temperature of polymerization. This phenomenon is due to increasing rates of chain transfer to monomer and aluminium. This is expected, since the relatively high activation energy of chain transfer becomes

attained by a greater proportion of the sample at high temperatures. It was noticed that the molecular weight distribution contained a small tail for low molecular weight. The size of the tail increased as the temperature increased (Figure 21). Comparing with **I**, the molecular weight was more strongly influenced by polymerization temperature for catalyst **II**, implying that chain transfer was more facilitated. This is ascribed to the difference in the nature of counter-ion, making transfer to aluminium much more likely for **II**, via contact ion pairs.

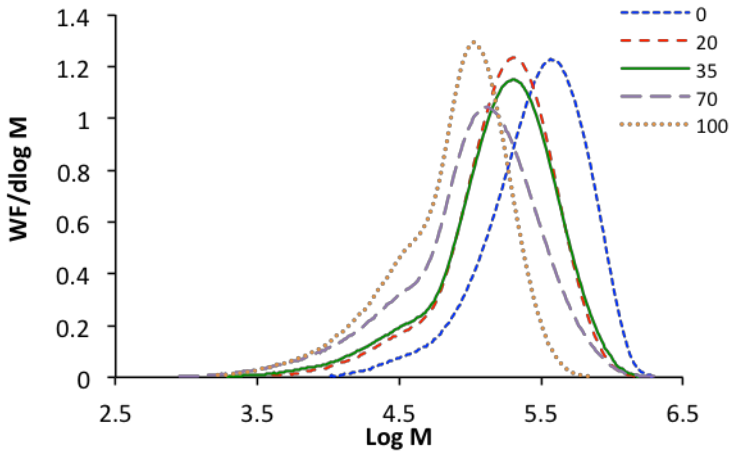

Figure 21 GPC curves of polyisoprene by II/DEAC at different temperature.

The counter-ion of **II** ($[Al]^-$) is tighter to the active centre and smaller compared to BArF. Therefore chain transfers are more facilitated resulting in lower M_n and a small molecular weight tail introduced to the molecular weight distribution.

6 Determination of the microstructure of polyisoprene

The obtained polyisoprene was characterized by $^{13}C\{^{1}H\}$NMR in order to investigate its microstructure according with the literature.[8, 9, 10] The spectra of two different samples with different microstructure are displayed in Figure 22-Figure 25. Polyisoprene obtained using catalyst **I** at 35 ˚C resulted in approximately 78% *cis*-1,4 enchainment, but there are also significant amounts of 3,4-vinyl and a very small amount of *trans*-1,4-enchained monomers, as shown by Figure 22 and Figure 23. The pattern of selectivity and regioerrors after 3,4 linkages are exactly as were reported for β-triketimine cobalt.[1] Eight distinct monomer triad environments are shown in Chart 2 and the most abundant triads would be **A** and **C**. Peaks are labelled according to this key Chart 2.

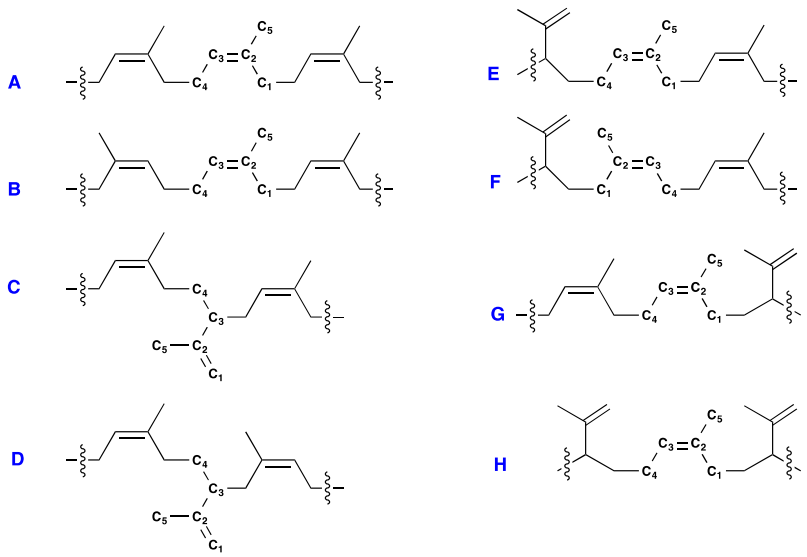

Chart 2 NMR Assignments for high-cis polymer (*trans* triads and consecutive 3,4 diads neglected).

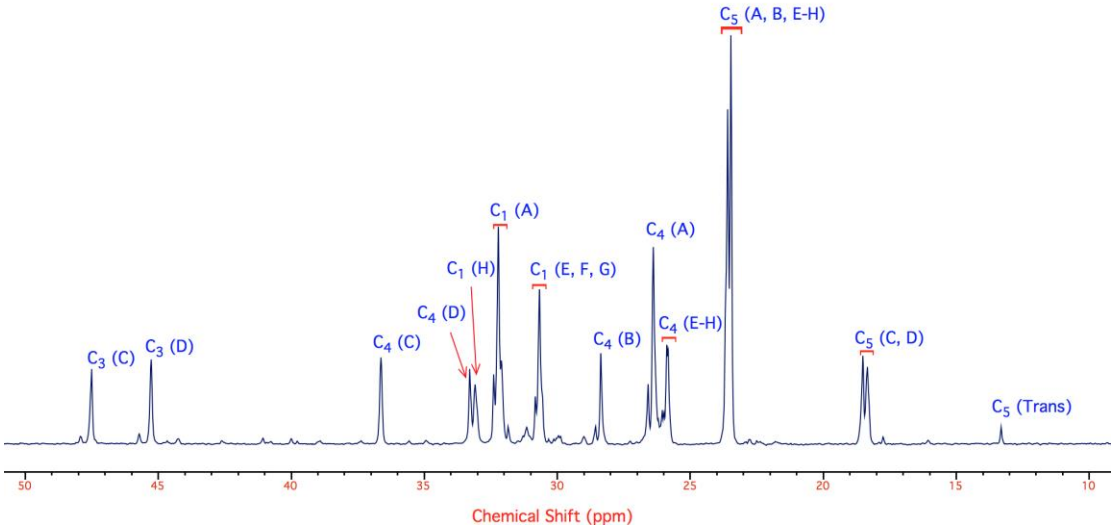

Figure 22 ^{13}C NMR spectrum (sp^3 region) of PI by I at 35 °C (*cis*-1.4 = 78.2%; *trans*-1,4 = 0.2%; 3,4 =21.6).

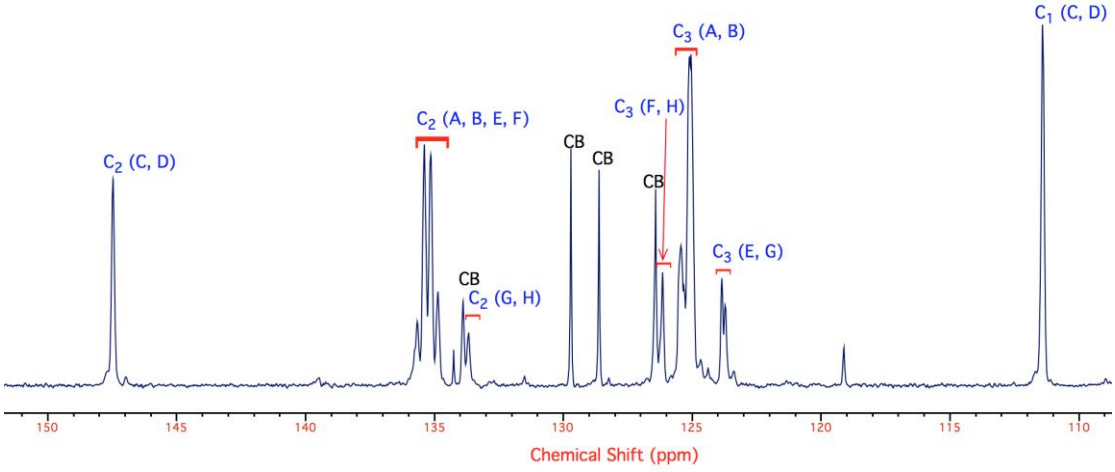

Figure 23 ^{13}C NMR spectrum (sp^2 region) of PI by I at 35 °C (*cis*-1.4 = 78.2%; *trans*-1,4 = 0.2%; 3,4 =21.6). CB is chlorobenzene (the polymerization solvent).

At lower polymerization temperature, the produced polymer was 43.0% *trans*-1.4, 42.2% *cis*-1,4 and 14.8 3,4 (Figure 24 and Figure 25). Assignment of the peaks in this high-*trans* polymer requires the definition of further triads incorporating *trans* units. Some of these are shown in Chart 3.

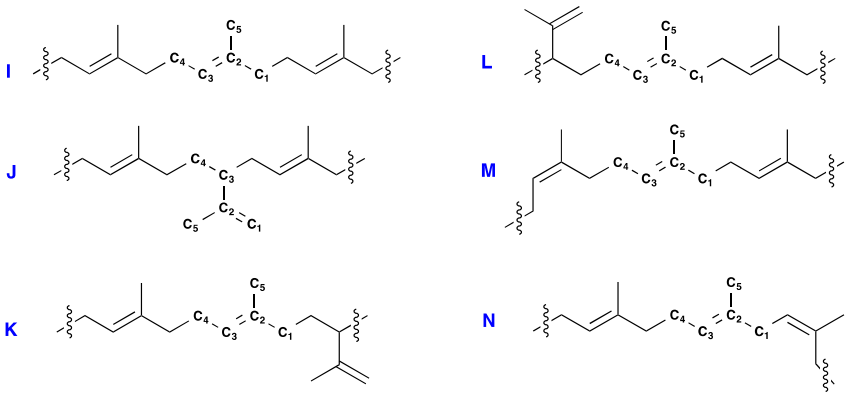

Chart 3 Polymer triads expected in a high-*trans* polyisoprene.

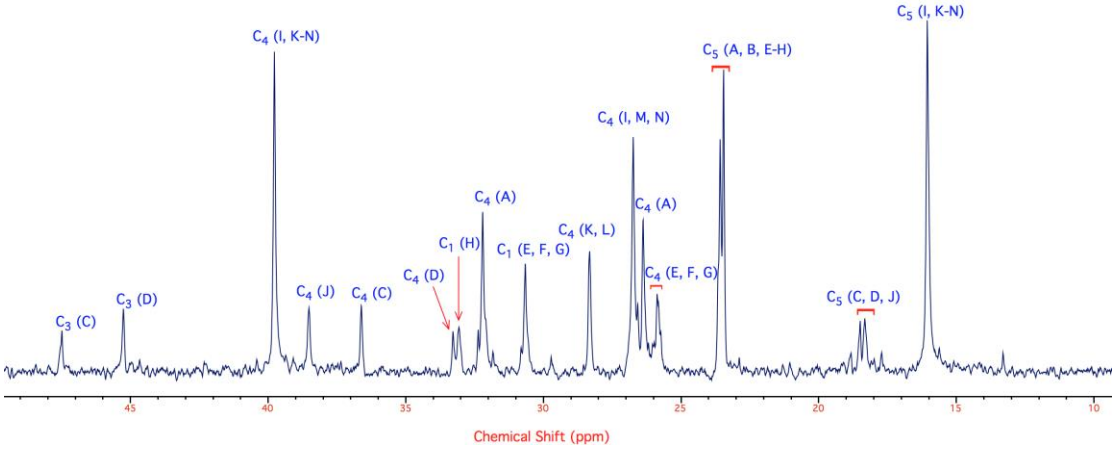

Figure 24 ^{13}C NMR spectrum (sp^3 region) of PI by I at 0 °C (*cis*-1,4 = 42.2%; *trans*-1,4 = 43.0%; 3,4 =14.8).

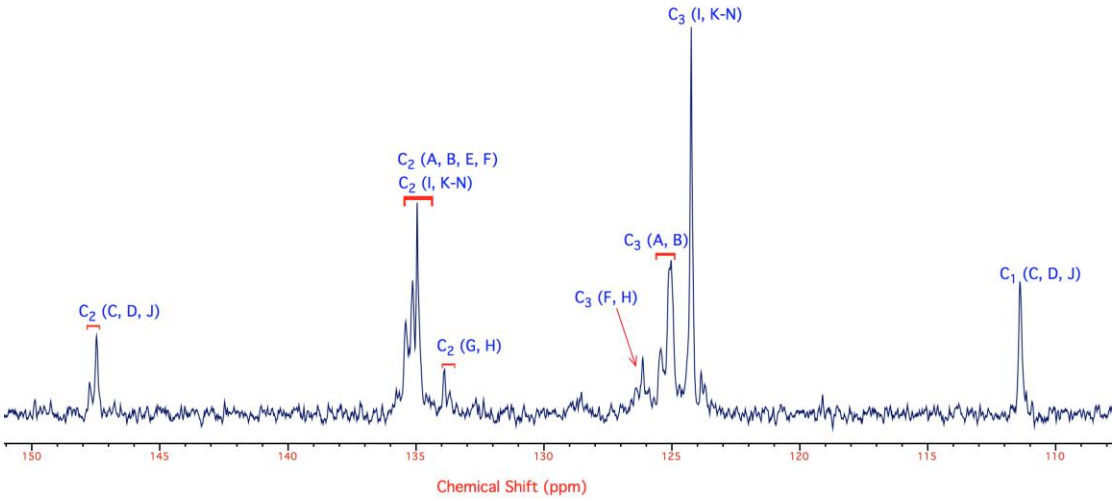

Figure 25 ^{13}C NMR spectrum (sp^2 region) of PI by I at 0 °C (*cis*-1,4 = 42.2%; *trans*-1,4 = 43.0%; 3,4 =14.8).

7 Crystallographic information

Table 1 Crystallographic information for I and II

Identification code	**I**	**II**
Empirical formula	$C_{70}H_{63}BBrCoF_{24}N_3O$	$C_{40}H_{47}Br_2Cl_2CoN_3$
Formula weight	1567.88	859.45
Temperature/K	150	150
Crystal system	monoclinic	monoclinic
Space group	C2/c	$P2_1/n$
a/Å	32.4767(19)	15.6906(11)
b/Å	12.0362(7)	14.9680(10)
c/Å	40.298(2)	17.0951(13)
α/°	90	90
β/°	114.988(7)	96.021(6)
γ/°	90	90
Volume/Å^3	14278.0(17)	3992.8(5)
Z	8	4
ρ_{calc}g/cm^3	1.459	1.430
μ/mm^{-1}	0.907	2.596
F(000)	6360.0	1756.0
Crystal size/mm^3	0.1 × 0.1 × 0.1	0.2 × 0.2 × 0.2
Radiation	MoKα (λ = 0.71073)	MoKα (λ = 0.71073)
2Θ range for data collection/°	6.066 to 52.744	6.562 to 57.428
Index ranges	-40 ≤ h ≤ 35, -10 ≤ k ≤ 15, -34 ≤ l ≤ 50	-21 ≤ h ≤ 20, -19 ≤ k ≤ 19, -21 ≤ l ≤ 20
Reflections collected	28116	17840
Independent reflections	14566 [R_{int} = 0.0356, R_{sigma} = 0.0719]	8966 [R_{int} = 0.0405, R_{sigma} = 0.0750]
Data/restraints/parameters	14566/0/920	8966/121/482
Goodness-of-fit on F^2	1.011	1.046
Final R indexes [I>=2σ (I)]	R_1 = 0.0689, wR_2 = 0.1344	R_1 = 0.0522, wR_2 = 0.1105
Final R indexes [all data]	R_1 = 0.1107, wR_2 = 0.1540	R_1 = 0.1060, wR_2 = 0.1293
Largest diff. peak/hole / e Å^{-3}	1.04/-1.06	0.89/-1.12

8 References

1. M. N. Alnajrani and F. S. Mair, *RSC Advances*, 2015, **5**, 46372.
2. F. Ghiotto, C. Pateraki, J. R. Severn, N. Friederichs and M. Bochmann, *Dalton Trans.*, 2013, **42**, 9040.
3. A. He, G. Wang, W. Zhao, X. Jiang, W. Yao and W.-H. Sun, *Polym. Int.*, 2013, **62**, 1758.
4. P. Cass, K. Pratt, T. Mann, B. Laslett, E. Rizzardo and R. Burford, *J. Polym Sci. A, Polym Chem*, 1999, **37**, 3277.
5. P. Ai, L. Chen, Y. Guo, S. Jie and B.-G. Li, *J. Organomet. Chem.*, 2012, **705**, 51.
6. S. Jie, P. Ai and B.-G. Li, *Dalton Trans.*, 2011, **40**, 10975.
7. H. Liu, X. Jia, F. Wang, Q. Dai, B. Wang, J. Bi, C. Zhang, L. Zhao, C. Bai, Y. Hu and X. Zhang, *Dalton Trans.*, 2013, **42**, 13723.
8. Y. Hu, W. Dong and T. Masuda, *Macromol. Chem. Phys.*, 2013, **214**, 2172.
9. Y. Hu, C. Zhang, X. Liu, K. Gao, Y. Cao, C. Zhang and X. Zhang, *J. Appl. Polym. Sci.*, 2014, **131**, 40153.
10. V. A. Rozentsvet, A. S. Khachaturov and V. P. Ivanova, *Polym. Sci Ser. A*, 2009, **51**, 870.